Advanced bismuth-doped lead-germanate glass for broadband optical gain devices

M. Hughes,* T. Suzuki, and Y. Ohishi

Toyota Technological Institute, 2-12, Hisakata, Tempaku, Nagoya 468-8511, Japan
**Corresponding author: mark@toyota-ti.ac.jp*

Received February 28, 2008; revised June 4, 2008; accepted June 15, 2008;
posted June 23, 2008 (Doc. ID 93173); published July 30, 2008

We fabricated a series of glasses with the composition 94.7-χGeO_2-5Al_2O_3-0.3Bi_2O_3-χPbO (χ=0–24 mol. %). Characteristic absorption bands of bismuth centered at 500, 700, 800, and 1000 nm were observed. Adding PbO was found to decrease the strength of bismuth absorption. The addition of 3%–4% PbO resulted in a 50% increase in lifetime, a 20-fold increase in quantum efficiency, and a 28-fold increase in the product of emission cross section and lifetime on the 0% PbO composition. We propose that the 800 nm absorption band relates a different bismuth center than the other absorption bands.

OCIS codes: 300.2530, 140.3380.

1. INTRODUCTION

The invention of the erbium doped fiber amplifier (EDFA) in 1987 [1] was instrumental in allowing long distance data transmission through silica fiber and was a significant improvement on electronic repeaters that required conversion between optical and electronic signals. By a quirk of nature an emission band of erbium, which dictates the gain bandwidth of the EDFA, sits neatly in the low-loss window of silica. The technology behind silica fiber is now mature; its structure and properties are well understood, and the loss achievable in silica fiber comes close to its theoretical minimum. Until recently the presence of the hydroxyl impurity in silica introduced an overtone absorption around 1400 nm that effectively divided the region of lowest attenuation into two separate windows. In 1998, Lucent Technologies introduced the AllWave fiber that contains less than 1 part in 10^9 hydroxyl ions. This ultradry fiber effectively gives one continuous low-loss window spanning ~1200–1600 nm. The gain bandwidth of the EDFA spans only a small fraction of this continuous low-loss window. Doping with other rare earths could allow wavelengths not covered by the EDFA to be used, but problems associated with the vibrational structure of silica prevent its use as an amplifier medium when doped with ions such as praseodymium, thulium, and dysprosium. Efficient optical amplification can be obtained from these dopants in nonoxide glass hosts; for instance, a praseodymium doped fiber amplifier with a signal gain of 40 dB at 1.3 μm [2] and a thulium doped fiber amplifier with a maximum gain of 28 and 35 dB at 1.47 [3] and 1.65 μm [4], respectively, have been demonstrated. However, the gain bandwidths of these devices are still relatively narrow, and they have poor compatibility with a silica based fiber. Fiber Raman amplifiers can achieve broadband amplification in silica glass; however, they require high pump powers and complex pumping schemes. One possible solution is to use a fiber amplifier doped with an ion that has a broad emission band that could replace or complement the EDFA. Transition metals are well known for their broad absorption and emission bands, for example, vanadium doped gallium-lanthanum-sulphide (V:GLS) glass displays emission centered at ~1500 nm with a full width at half-maximum (FWHM) of ~500 nm [5]. However, similar to other transition metal doped glasses, V:GLS has a relatively low quantum efficiency (QE) and a lifetime of 4% and 30 μs, respectively; this indicates that it may have a high laser threshold.

Recently, Fujimoto and Nakatsuka [6,7] discovered a new broadband infrared emission from bismuth-doped silica glass and demonstrated 1300 nm optimal amplification with 800 nm excitation. Later, bismuth-doped glasses started to attract much attention since Dianov *et al.* [8] demonstrated laser action between 1150 and 1300 nm in a bismuth-doped aluminosilicate fiber. Ultrabroad emission with an FWHM of ~600 nm has also been observed in a bismuth-doped soda-lime-silicate glass [9]. This implies the exciting possibility of developing a broadband optical fiber amplifier based on bismuth-doped glass for use in fiber optic communications that could overcome the problem of limited gain bandwidth of the EDFA. The optical properties of a variety of bismuth-doped glasses including GeO_2-SrO-Al_2O_3 [10], Li_2O-Al_2O_3-SiO_2 [11], and B_2O_3-BaO-Al_2O_3 [12] have been investigated. Of these, germanate glasses are particularly attractive because optical amplification has been demonstrated in them [13], and the change of host from silica to germanium can greatly enhance the transmittance of the glass and reduce the melting temperature [14]. It has been reported that the maximum transmission of bismuth-doped silicate glass, prepared by the conventional melt-quench technique, was 30% in a 2 mm thick sample; this was due to bubbles in the glass [6]. For the bismuth-doped lead-germanate glass in this paper; we found a maximum transmission of 80% in a 5 mm thick sample. In bismuth-

doped crystals, assignment of the bismuth oxidation state has generally been made unambiguously. In bismuth-doped glasses near-infrared emission has often been observed; however, there is a lot of uncertainty as to the oxidation state of bismuth in glasses, and most of the oxidation state assignments were made tentatively. The near-infrared emission of bismuth-doped glasses has been attributed to Bi^{+} [12], Bi^{5+} [6,15], and bismuth metal clusters [16].

In this paper we demonstrate an improvement to the Bi_2O_3 doped GeO_2-Al_2O_3 (GAB) glass system, in which broadband optical amplification has already been demonstrated [13], through the addition of PbO, which is now referred to as GAPB glass. To the best of our knowledge this paper is the first time the optical properties of bismuth-doped lead-germanate glass have been reported and the first time the QE as a function of glass composition for a bismuth-doped glass has been reported. We initially tried reproducing the GAB glass reported in [13]. After finding that the bismuth appeared to be inhomogeneously distributed we tried various codopants including LiO and PbO to improve this. Both of these codopants improved the homogeneity; however, LiO reduced the emission intensity, whereas PbO increased it and gave an unexpected color change. This led to the experiments reported in this paper. In this paper we measured the absorption, emission, and lifetime of 16 samples with PbO contents between 0% and 24% at excitation wavelengths of 514, 700, 800, and 974 nm. For the sake of clarity and a practical number of figures we have shown different PbO content glasses in the various figures in order to highlight the trends we observed.

2. EXPERIMENTAL

A. Glass Melting

GAB and GAPB glasses were prepared by mixing 94.7-$\chi$$GeO_2-5Al_2O_3-0.3Bi_2O_3$-$\chi$PbO ($\chi$=0–24 mol. %) in a dry-nitrogen-purged glove box. The glasses were then melted in an electrical furnace, with an N_2 atmosphere, in alumina crucibles. Subsequently the glass melts were quenched by pouring them onto stainless steel plates preheated to 450°C. Each glass was then annealed at 600°C for 3 h. Finally the glasses were cut to a size of around 20 mm × 20 mm × 2.5 mm and then well polished with progressively finer wet polishing paper. The melting temperature for the 0% PbO (GAB) glass was 1540°C. The melting temperature for the 24% PbO glass was 1200°C, rising to 1370°C for the 2% PbO glass. However, differential thermal analysis (DTA) of the glasses indicated that the melting temperature for all the PbO containing glasses was around 1170°C. The increase in melting temperature with a decreasing PbO content was necessary to facilitate pouring of the glass, since the viscosity of the glass increased significantly with a decreasing PbO content. Glasses with 0% PbO were dark brown in appearance; with PbO concentrations up to 3%, the glasses were an opaque dark pink. Glasses with a 4%–12% PbO content were a translucent pale pink, which became progressively paler with an increasing PbO content. Above 12% the PbO content of all the glasses appeared colorless. We chose a fixed composition of 5% Al_2O_3 in this paper because this has been shown to maximize the emission lifetime and intensity in GAB glass [17].

B. Spectroscopic Measurements

Absorption spectra were taken on a PerkinElmer Lambda 900 spectrophotometer over a range of 175–3300 nm with a resolution of ±0.1 nm. Various laser sources were used to obtain photoluminescence (PL) spectra: a 974 nm Furakawa laser diode, a Coherent 890 Ti:sapphire laser tuned to 700 or 800 nm, and a Spectra-Physics argon ion laser tuned to 514 nm. The 974 nm laser source was electronically modulated, giving a $1/e$ fall time of ~250 ns, whereas the 514, 700, and 800 nm laser sources were focused with a microscope objective and modulated with a mechanical chopper at the focus waist, which gave a $1/e$ fall time of ~50 μs. PL spectra were obtained by dispersing the fluorescence generated by laser sources in a Jasco CT-25C monochromator that used a 600 lines/mm grating blazed at 1000 nm; the slit width was ~1 mm that corresponded to a resolution of ~10 nm. The 974 nm excitation was blocked with a 980 nm notch filter, and the 514, 700, and 800 nm excitation was blocked with an 850 nm long pass filter. Detection was realized with a Hamamatsu H9170 NIR photomultiplier tube (PMT), with a fall time of 1.7 ns, coupled with standard phase sensitive detection. All spectral measurements were corrected for the wavelength dependent response of the measurement system by calculating a correction spectra [$C(\lambda)$] with $C(\lambda) = I_{cal}(\lambda)/I_{meas}(\lambda)$, where $I_{meas}(\lambda)$ is the luminescence spectrum of an Ushio calibrated white light source measured by the detection system, and $I_{cal}(\lambda)$ is the luminescence spectrum of the calibrated white light source supplied by the manufacturer. Transient fluorescence measurements were made with the same system used for spectral measurements, except the transient signal was captured with a Yokogawa DL1620 200 MHz oscilloscope and averaged ~10,000 times.

QE measurements were taken with the same system used for spectral measurements, except the samples with dimensions of ~3 mm × 3 mm × 1 mm were placed in a Labsphere 4P-GPS-040-SF integrating sphere with a diameter of ~10 cm, and the signal was detected with a Hamamatsu G5852-11 InGaAs detector. The samples were mounted behind a baffle such that there was no direct line-of-sight between the sample and the exit port and angled such that reflected excitation light was directed away from the entrance port. A "photons out/photons in" method similar to that described in [18,19] for calculating the QE was used. The number of photons absorbed was taken to be proportional to the difference between the area under the laser line spectra with the sample present [$I_{sample}(\lambda)$] and without the sample present [$I_{sphere}(\lambda)$]. The number of photons emitted was taken to be proportional to the area under the emission spectra [$I_{PL}(\lambda)$]. The spectra were corrected with a correction spectra [$C(\lambda)$]. A correction for photon energy was also made since a higher photon flux is required at longer wavelengths to produce the same irradiance per unit area as at shorter wavelengths by multiplying by the wavelength. Hence the QE (η_{QE}) was calculated with

$$\eta_{QE} = \frac{\int \lambda I_{PL}(\lambda) C(\lambda) d\lambda}{\int \lambda I_{sphere}(\lambda) C(\lambda) d\lambda - \int \lambda I_{sample}(\lambda) C(\lambda) d\lambda}. \quad (1)$$

There was found to be a lot of variability in the QE measurements of the weakly absorbing samples; this was caused by difficulty in measuring the amount of excitation laser light that was absorbed. To overcome this, laser line spectra were taken up to ten times for each QE measurement and 10–15 QE measurements were made for each sample, totaling ~1500 spectra for the QE measurements in this paper. Differential scanning callorimetry (DSC) measurements were made with a Rigaku Thermoplus DSC 8270. Refractive index measurements were made with a Metricon 2010 prism coupler.

3. RESULTS AND DISCUSSION

A. Absorption Measurements

Figure 1 shows the absorption spectra of some GAPB glasses with various PbO concentrations. Four main absorption bands centered around 500, 700, 800, and 1000 nm are identified, which is similar to the characteristic bismuth absorption observed in other glasses [10,11,20]. It can be seen that as the PbO content increases the absorption bands attributed to bismuth tend to decrease in strength. This might occur because the addition of PbO may permit the bismuth dopant to be incorporated as a structural component of the glass, rather than an optically active ion, since many authors have proposed a structural similarity between lead-rich and bismuth-rich glasses [21]. It is also noted that the transparency of the glass increases with an increasing PbO content.

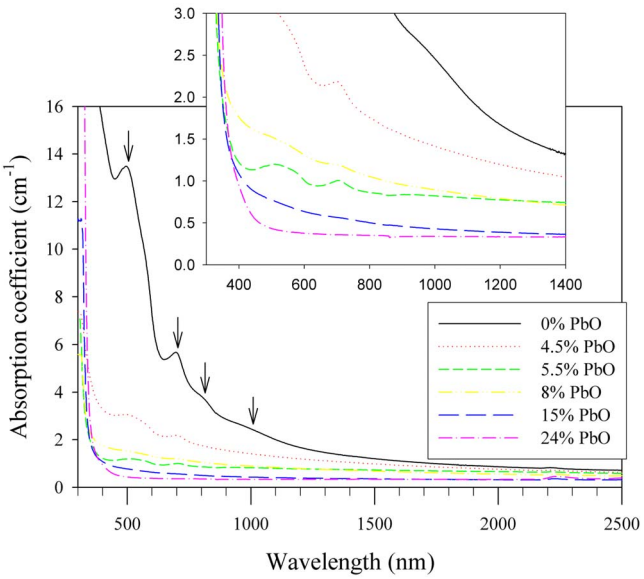

Fig. 1. (Color online) Absorption spectra of GAPB glasses with various PbO concentrations. The identified bismuth absorption bands are indicated with arrows. Inset shows a close-up of the weakly absorbing samples.

B. Emission Spectra Measurements

Figure 2(a) shows the PL spectra of some GAPB glasses with various PbO concentrations taken using a 974 nm laser excitation source. One main emission band can be observed centered at ~1100 nm; this emission band is observed in all the glasses except the 24% PbO glass. A weaker emission band that peaks between 1330 and 1475 nm and varies in relative intensity with the PbO content of the glass is also observed. A 1330 nm emission band is apparent in the 0% PbO content glass, which then fades in glasses with a 2%–10% PbO content. As the PbO content is increased past 10% (not shown for clarity) an emission band peaking at 1475 nm is observed; the intensity of this band steadily increases with the PbO content. In Fig. 2(b) the emission spectrum of the 0% PbO content glass has been deconvoluted with two Gaussians. The fit of the two Gaussians, which are centered at 1090 and 1330 nm, is very consistent with the observed spectrum. Emission peaks at 1100 and 1350 nm have also been observed in bismuth-doped Li_2O-Al_2O_3-SiO_2 glass under 900 nm excitation [11]; however, the 1350 nm band was almost as intense as the 1100 nm band. The deconvolution of the emission spectrum of the 22% PbO glass (not shown) revealed two Gaussians centered at 1110 and 1475 nm; however, it is unclear if this 1475 nm emission band is a re-emergence of the 1330 nm emission band observed in the 0% PbO content glass that has been redshifted or a separate emission band related to a different phenomenon. Increasing the PbO content from 22% to 24% causes the emission spectra to undergo a dramatic

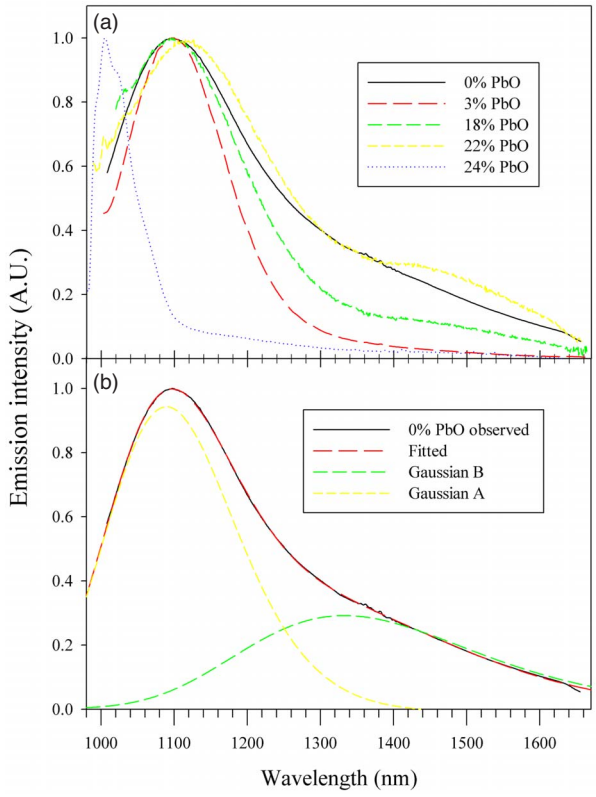

Fig. 2. (Color online) (a) PL spectra, excited at 974 nm, of GAPB glasses with various PbO concentrations. (b) Deconvolution of the emission spectrum of the glass with a 0% PbO content with two Gaussians.

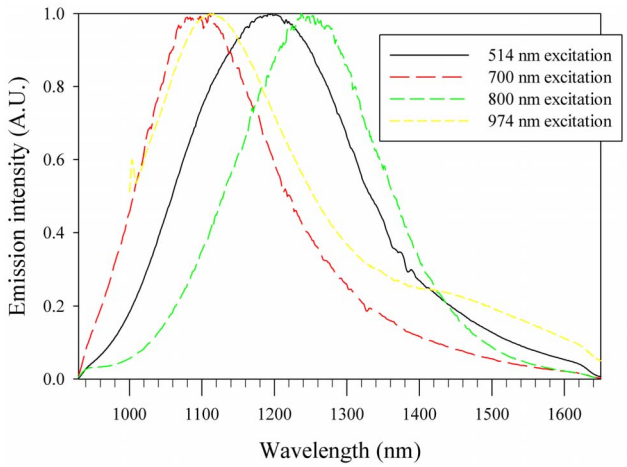

Fig. 3. (Color online) PL spectra, excited at 514, 700, 800, and 974 nm, of GAPB glasses with a 20% PbO content.

change. The peak shifts from 1100 to 1000 nm and the width decrease sharply. It is noteworthy that this dramatic change in emission occurs at 24% PbO, where the GeO_2-PbO ratio is 2.95 since a GeO_2-PbO ratio of near 3 has been identified as an optimum ratio for stable glass formation by analysis of the phase diagram of the GeO_2-PbO binary system [22]. We therefore tentatively suggest that a phase change is responsible for the change in emission spectrum.

Figure 3 shows the bismuth emission spectra from a 20% PbO sample, excited at wavelengths of 514, 700, 800, and 974 nm, which roughly equates to exciting into each of the four absorption bands identified in Fig. 1. It appears that 700 nm excitation activates the same characteristic 1100 nm emission band as 974 nm excitation, but the 1475 nm emission band is less apparent. The emission spectra from 700 nm excitation for PbO concentrations of 0% to 24% (not shown) were roughly similar to the spectrum in Fig. 3. Excitation at 800 nm appears to activate a single 1250 nm emission band; this is similar to the emission observed from $75B_2O_3$-20BaO-$5Al_2O_3$-$2Bi_2O_3$ glass under 808 nm excitation [12]. Under 514 nm excitation a 1200 nm emission band is observed. In the emission spectra from 514 nm excitation for PbO concentrations of 2%–10% (not shown) a single 1100 nm emission band was observed, which was broadly similar to the emission spectra for 700 and 974 nm excitation shown in Fig. 3.

Figure 4 shows how the width of emission varies as a function of the PbO content for the different pump wavelengths. Excitation at 974 and 700 nm gives similar dependencies on the PbO content as do 800 and 514 nm excitation. For 974 nm excitation the addition of PbO initially reduces the emission width from GAB glass, where it remains constant until ~12% PbO, after which it steadily increases to reach a maximum at ~22% PbO.

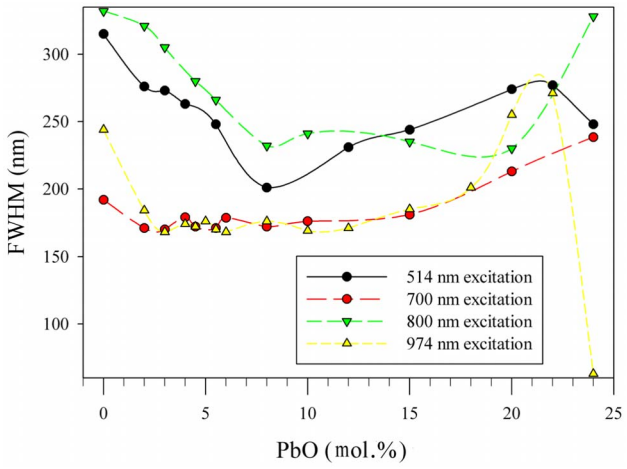

Fig. 4. (Color online) Emission FWHM as a function of the PbO content for various excitation wavelengths. Curves are a guide for the eye.

C. Emission Lifetime Measurements

Figure 5 shows the emission decay profiles of GAPB glasses with 3% and 22% PbO contents. The fluorescence decay profiles were found to be nonexponential but could be accurately described using the stretched exponential function

$$I(t) = y_0 + I_0 \exp\left(-\left(\frac{t}{\tau_0}\right)^{\beta}\right), \tag{2}$$

where I_0 is the initial fluorescence intensity, y_0 is the offset, τ_0 is the characteristic fluorescence lifetime, and β is the stretch factor. The closer β is to zero the more the function deviates from a single exponential. The stretched exponential function has been shown to describe many relaxation processes in amorphous and crystalline materials, such as nuclear relaxation [23], magnetic susceptibility relaxation [23], fluorescence decay [5,24–28], and photoinduced dichroism [29]. Though stretched exponential behavior has been observed in many relaxation processes, particularly in disordered materials such as glasses, there has been considerable debate as to the physical interpretation of the characteristic lifetime τ_0 and stretch factor β. Stretched exponential relaxation is commonly interpreted as a sum of pure exponential decays with a probability distribution P of τ lifetime values for a given value of β [30]. Recently, the probability distribution $P(\tau_0/\tau)$ of the stretched exponential function for different β values have been calculated [30–32]. Analysis of these distributions leads to the following physical inter-

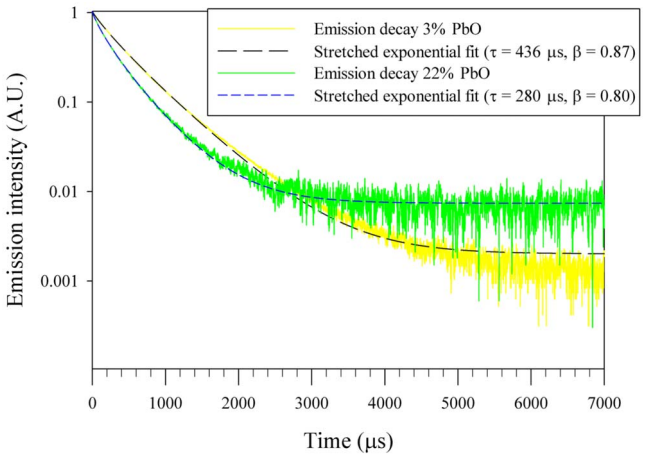

Fig. 5. (Color online) Emission decay profiles of GAPB glasses with PbO contents of 3% and 22%.

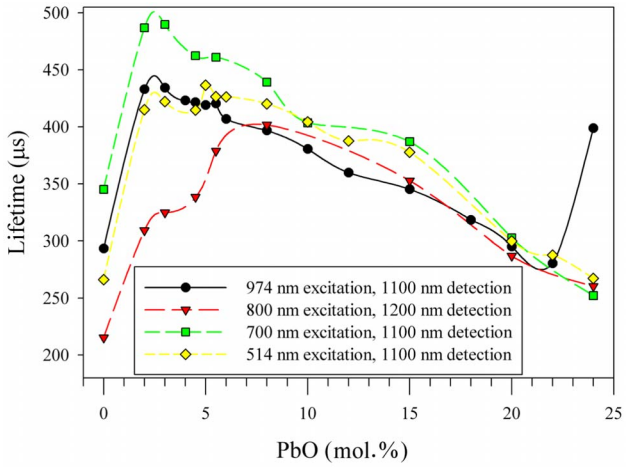

Fig. 6. (Color online) Emission lifetime, detected at the emission peak, as a function of the PbO content for excitation wavelengths of 514, 700, 800, and 974 nm. Curves are a guide for the eye.

pretations: that τ_0 is that τ, which is equally likely to be less than τ_0 as it is to be greater, and that β is a measure of the intrinsic long lifetime cutoff of $P(\tau_0/\tau, \beta)$ [30].

Figure 6 shows the emission lifetime measured at approximately the peak of the emission. For 974 nm excitation there is an initial 50% increase in lifetime with the addition of PbO that then steadily decreases to approximately the 0% PbO value at 22% PbO, before increasing again at 24% PbO. There is a very similar trend for 700 nm excitation, with the exception of 24% PbO, which has already been identified as a special case. The trend for 514 nm excitation is similar to the trend for 700 and 974 nm excitation but with longer lifetimes. However, the trend for 800 nm excitation is different from other excitation wavelengths with the maximum lifetime occurring at ~10% PbO.

Figure 7 shows the detection wavelength-dependent lifetime of the 5% PbO content glass at the four different excitation wavelengths. The trends for 514, 700, and 974 nm excitation follow a broadly similar pattern with the maximum lifetime occurring at slightly longer wavelengths than the maximum emission intensity; the lifetime then reaches a minimum at around 1400 nm and then increases at longer wavelengths. For 800 nm excitation the general trend is for a steadily increasing lifetime with an increasing detection wavelength, with a small increase close to the emission peak at 1250 nm.

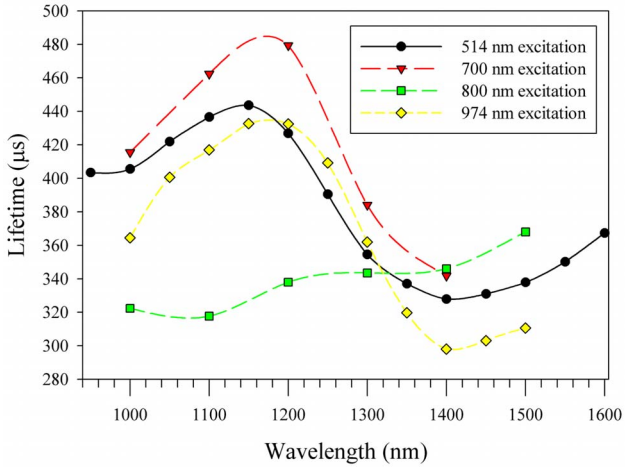

Fig. 7. (Color online) Lifetime spectra of 5% PbO GAPB glass for excitation wavelengths of 514, 700, 800, and 974 nm. Curves are a guide for the eye.

D. Quantum Efficiency Measurements

Figure 8 shows the QE of GAPB glasses, excited at 974 nm, as a function of the PbO content of the glass. The error bars show one standard deviation from the mean. We chose to use 974 nm excitation for the QE measurements because broadband optical amplification has been demonstrated in GAB glass using 974 nm excitation [13]. Figure 8 also shows the product of the peak emission cross section and the emission lifetime ($\sigma_{em}\tau$), which is an important parameter for a gain medium since it is inversely proportional to the laser threshold [33]. The peak emission cross section (σ_{em}) was estimated from the Füchtbauer–Landenburg equation by assuming a Gaussian-shaped emission band [34] and is given by

$$\sigma_{em} = \sqrt{\frac{\ln 2}{\pi}} \frac{\lambda_0^2}{4\pi n^2 \tau_{rad} \Delta v}, \tag{3}$$

where λ_0 is the peak emission wavelength, Δv is the FWHM of the emission in units of energy, n is the refractive index, c is the speed of light, and τ_{rad} is the radiative lifetime calculated from the measured lifetime (τ) by $\tau_{rad} = \tau/\mathrm{QE}$. Figure 8 shows that the QE has a similar dependence on the PbO content as the lifetime. This indicates that the radiative rate remains constant, and the nonradiative rate increases as the PbO content is increased; this could be caused by an increase in maximum phonon energy as the PbO content is increased. An increase in maximum phonon energy would increase the probability of nonradiative decay by decreasing the number of phonons required for a multiphonon emission process. The QE has a peak of ~60% at ~4% PbO; this represents a 20-fold increase in QE on GAB glass. These QE measurements compare to 11% for bismuth doped Li_2O-Al_2O_3-SiO_2 glass when excited at 974 nm [35]. Considering how the emission spectra changes as a function of the PbO content, it appears that when the long wave-

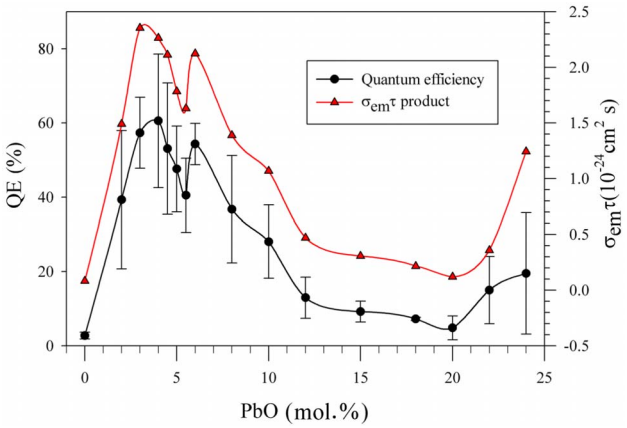

Fig. 8. (Color online) QE and $\sigma_{em}\tau$ as a function of the PbO content. Curves are a guide for the eye.

length component of the emission is present, as in 0% and 10%–22% PbO, the QE is reduced. Comparing Figs. 4, 6, and 8 indicates that an increase in lifetime and QE occurs with a narrowing emission width. The $\sigma_{em}\tau$ product has a peak of $\sim 2.4\times10^{-24}$ cm^2 s at $\sim$3% PbO; this represents a 28-fold increase on GAB glass. However, glass at this composition has low transparency and is difficult to prepare; further development of the glass fabrication process could overcome this, but as a compromise $89GeO_2$-$6PbO$-$5Al_2O_3$-$0.3Bi_2O_3$ glass is suggested for further development as a gain medium. The peak $\sigma_{em}\tau$ of $\sim 2.4\times10^{-24}$ cm^2 s declared in this paper is slightly lower than the $\sigma_{em}\tau$ for bismuth emission reported by other authors: 5.1×10^{-24} cm^2 s for bismuth-doped Na_2O-CaO-MgO-Al_2O_3-SiO_2 glass [9], 6.1×10^{-24} cm^2 s for bismuth-doped Li_2-Al_2O_3-SiO_2 glass [11], 4.2×10^{-24} cm^2 s for bismuth-doped GeO_2-Al_2O_3 glass [17], and 6.1×10^{-24} cm^2 s for bismuth-doped GeO_2-Al_2O_3-Na_2O glass [15]. The $\sigma_{em}\tau$ reported by these authors was calculated using a similar method to this paper; however, the measured lifetime rather that the radiative lifetime was used. These reports may therefore be an overestimate if the QE is less than 100%.

Since optical gain of 3.65 dB at 1270 nm under 974 nm excitation has been demonstrated in GAB glass [13], the 27-fold increase in $\sigma_{em}\tau$ obtained with the addition of 3% PbO to GAB glass is highly significant because it implies that a much larger optical gain could be demonstrated in the glass; this will be the subject of further work after additional enhancement of the glass composition and fabrication process.

4. MODEL OF EMISSION

The following differences have been observed between the emission properties of the 800 nm absorption band to the 500, 700, and 1000 nm absorption bands.

- Emission peaking at 1250 nm rather than 1100 nm.
- Different dependence of emission FWHM as a function of the PbO content.
- Different trend in emission lifetime as a function of the PbO content.
- Different dependence of lifetime as a function of the emission wavelenth.

The different emission wavelength and the different lifetime dependence of the emission wavelength (Fig. 7) indicate that the 1250 nm emission band observed under 800 nm excitation is a different emission band to the 1330 nm emission band observed under 974 nm excitation [Fig. 2(b)]. The fact that the 1250 nm emission band, observed under 800 nm excitation, is present in all PbO content glasses, whereas the 1330 nm emission band observed under 974 nm excitation is observed only in the 0% PbO glass, also backs up this hypothesis. We therefore propose that the 500, 700, and 1000 nm absorption bands are associated with the same bismuth emission center (emission center *A*) and the 800 nm absorption band is associated with a different emission center (emission center *B*). However, because there are some similarities between the 500 and 800 nm absorption bands such as the longer emission wavelength at certain PbO concentrations under 514 nm excitation, and in the emission FWHM as a function of the PbO content, we propose that emission center *B* may also accommodate a 500 nm absorption band.

5. CONCLUSIONS

The characteristic absorption bands of bismuth, centered at 500, 700, 800, and 1000 nm, were observed in bismuth-doped GAB and GAPB glass. The addition of PbO to GAB glass was found to decrease the strength of the absorption bands attributed to bismuth; this indicates that PbO helps bismuth to be incorporated into the glass in an optically inactive form. Four emission bands at 1005, 1100, 1330, and 1475 were observed with 974 nm excitation in GAPB glasses with a PbO content of 0%–24%. Excitation into the 500, 700, and 1000 nm absorption bands yielded broadly similar emission spectra and lifetime properties as a function of the PbO content of the glass; it is therefore suggested that these absorption bands belong to the same bismuth emission center. Because some fundamental differences were observed in the emission spectra and lifetime properties as a function of PbO when exciting into the 800 nm absorption band, it is suggested that this absorption band belongs to a separate bismuth emission center. We made a detailed measurement of the QE of GAPB glass as a function of the PbO content; to the best of our knowledge this is the first compositional dependent QE measurement for a bismuth-doped glass. The addition of the appropriate proportion of PbO to GAB glass resulted in a 50% increase in lifetime, a 20-fold increase in QE, and a 28-fold increase in $\sigma_{em}\tau$.

REFERENCES

1. R. J. Mears, L. Reekie, I. M. Jauncey, and D. N. Payne, "Low-noise erbium-doped fiber amplifier operating at 1.54 μm," Electron. Lett. **23**, 1026–1028 (1987).
2. M. Yamada, M. Shimizu, T. Kanamori, Y. Ohishi, Y. Terunuma, K. Oikawa, H. Yoshinaga, K. Kikushima, Y. Miyamoto, and S. Sudo, "Low-noise and high-power Pr3+-doped fluoride fiber amplifier," IEEE Photonics Technol. Lett. **7**, 869–871 (1995).
3. T. Komukai, T. Yamamoto, T. Sugawa, and Y. Miyajima, "Upconversion pumped thulium-doped fluoride fiber amplifier and laser operating at 1.47 μm," IEEE J. Quantum Electron. **31**, 1880–1889 (1995).
4. T. Sakamoto, M. Shimizu, M. Yamada, T. Kanamori, Y. Ohishi, Y. Terunuma, and S. Sudo, "35-dB gain Tm-doped ZBLYAN fiber amplifier operating at 1.65 μm," IEEE Photonics Technol. Lett. **8**, 349–351 (1996).
5. M. Hughes, H. Rutt, D. Hewak, and R. Curry, "Spectroscopy of vanadium (III) doped gallium lanthanum sulphide glass," Appl. Phys. Lett. **90**, 031108 (2007).
6. Y. Fujimoto and M. Nakatsuka, "Infrared luminescence from bismuth-doped silica glass," Jpn. J. Appl. Phys., Part 2 **40**, L279–L281 (2001).
7. Y. Fujimoto and M. Nakatsuka, "Optical amplification in bismuth-doped silica glass," Appl. Phys. Lett. **82**, 3325–3326 (2003).
8. E. M. Dianov, V. V. Dvoyrin, V. M. Mashinsky, A. A. Umnikov, M. V. Yashkov, and A. N. Gur'yanov, "CW bismuth fibre laser," Quantum Electron. **35**, 1083–1084 (2005).
9. Y. Arai, T. Suzuki, Y. Ohishi, S. Morimoto, and S. Khonthon, "Ultrabroadband near-infrared emission from a colorless bismuth-doped glass," Appl. Phys. Lett. **90**, 261110 (2007).
10. J. Ren, J. Qiu, B. Wu, and D. Chen, "Ultrabroad infrared

luminescence from Bi-doped alkaline earth metal germanate glasses," J. Mater. Res. **22**, 1574–1577 (2007).
11. T. Suzuki and Y. Ohishi, "Ultrabroadband near-infrared emission from Bi-doped Li_2O-Al_2O_3-SiO_2 glass," Appl. Phys. Lett. **88**, 191912 (2006).
12. X.-G. Meng, J.-R. Qiu, M.-Y. Peng, D.-.P Chen, Q.-Z. Zhao, X.-W. Jiang, and C.-S. Zhu, "Infrared broadband emission of bismuth-doped barium-aluminum-borate glasses," Opt. Express **13**, 1635–1642 (2005).
13. S. Zhou, H. Dong, H. Zeng, G. Feng, H. Yang, B. Zhu, and J. Qiu, "Broadband optical amplification in Bi-doped germanium silicate glass," Appl. Phys. Lett. **91**, 061919 (2007).
14. M. Peng, J. Qiu, D. Chen, X. Meng, I. Yang, X. Jiang, and C. Zhu, "Bismuth and aluminium codoped germanium oxide glasses for super-broadband optical amplification," Opt. Lett. **29**, 1998–2000 (2004).
15. X. Wang and H. Xia, "Infrared superbroadband emission of Bi ion doped germanium-aluminum-sodium glass," Opt. Commun. **268**, 75–78 (2006).
16. M. Peng, J. Qiu, D. Chen, X. Meng, and C. Zhu, "Superbroadband 1310 nm emission from bismuth and tantalum codoped germanium oxide glasses," Opt. Lett. **30**, 2433–2435 (2005).
17. M. Peng, C. Wang, D. Chen, J. Qiu, X. Jiang, and C. Zhu, "Investigations on bismuth and aluminum co-doped germanium oxide glasses for ultra-broadband optical amplification," J. Non-Cryst. Solids **351**, 2388–2393 (2005).
18. C. E. Finlayson, A. Amezcua, P. J. Sazio, P. S. Walker, M. C. Grossel, R. J. Curry, D. C. Smith, and J. J. Baumberg, "Infrared emitting PbSe nanocrystals for telecommunications window applications," J. Mod. Opt. **52**, 955–964 (2005).
19. N. C. Greenham, "Measurement of absolute photoluminescence quantum efficiencies in conjugated polymers," Chem. Phys. Lett. **241**, 89–96 (1995).
20. M. Peng, C. Wang, D. Chen, J. Qiu, X. Jiang, and C. Zhu, "Investigations on bismuth and aluminum co-doped germanium oxide glasses for ultra-broadband optical amplification," J. Non-Cryst. Solids **351**, 2388–2393 (2005).
21. V. N. Sigaev, I. Gregora, P. Pernice, B. Champagnon, E. N. Smelyanskaya, A. Aronne, and P. D. Sarkisov, "Structure of lead germanate glasses by Raman spectroscopy," J. Non-Cryst. Solids **279**, 136–144 (2001).
22. J. Wang, J. R. Lincoln, W. S. Brocklesby, R. S. Deol, C. J. Mackechnie, A. Pearson, A. C. Tropper, D. C. Hanna, and D. N. Payne, "Fabrication and optical properties of lead-germanate glasses and a new class of optical fibers doped with Tm^{3+}," J. Appl. Phys. **73**, 8066–8075 (1993).
23. J. C. Phillips, "Stretched exponential relaxation in molecular and electronic glasses," Rep. Prog. Phys. **59**, 1133–1207 (1996).
24. K. C. B. Lee, J. Siegel, S. E. D. Webb, S. Leveque-Fort, M. J. Cole, R. Jones, K. Dowling, M. J. Lever, and P. M. W. French, "Application of the stretched exponential function to fluorescence lifetime imaging," Biophys. J. **81**, 1265–1274 (2001).
25. R. A. L. Vallée, M. Cotlet, J. Hofkens, F. C. D. Schryver, and K. Mullen, "Spatially heterogeneous dynamics in polymer glasses at room temperature probed by single molecule lifetime fluctuations," Macromolecules **36**, 7752–7758 (2003).
26. G. Mauckner, K. T. T. Baier, T. Walter, and F. L. Sauer, "Temperature dependent lifetime distribution of the photoluminescence S-band in porous silicon," J. Appl. Phys. **75**, 4167–4170 (1993).
27. R. Chen, "Apparent stretched-exponential luminescence decay in crystalline solids," J. Lumin. **102–103**, 510–518 (2003).
28. J. Wlodarczyk and B. Kierdaszuk, "Interpretation of fluorescence decays using a power-like model," Biophys. J. **85**, 589–598 (2003).
29. A. B. Seddon, D. Furniss, M. S. Iovu, S. D. Shutov, N. N. Syrbu, A. M. Andriesh, P. Hertogen, and G. J. Adriaenssens, "Optical absorption and visible luminescence in Ga-La-S-O glass doped with Pr3+ ions," J. Optoelectron. Adv. Mater. **5**, 1107–1113 (2003).
30. D. C. Johnston, "Stretched exponential relaxation arising from a continuous sum of exponential decays," Phys. Rev. B **74**, 184430 (2006).
31. P. Hetman, B. Szabat, K. Weron, and D. Wodzinski, "On the Rajagopal relaxation-time distribution and its relationship to the Kohlrausch–Williams–Watts relaxation function," J. Non-Cryst. Solids **330**, 66–74 (2003).
32. I. Svare, S. W. Martin, and F. Borsa, "Stretched exponentials with T-dependent exponents from fixed distributions of energy barriers for relaxation times in fast-ion conductors," Phys. Rev. B **61**, 228–233 (2000).
33. S. Kuck, K. Peterman, U. Pohlmann, and G. Huber, "Near-infrared emission of Cr^{4+} doped garnates: lifetimes quantum efficiencies and emission cross sections," Phys. Rev. B **51**, 17323–17331 (1995).
34. X.-G. Meng, J.-R. Qiu, M.-Y. Peng, D.-P. Chen, Q.-Z. Zhao, X.-W. Jiang, and C.-S. Zhu, "Near infrared broadband emission of bismuth-doped aluminophosphate glass," Opt. Express **13**, 1628–1634 (2005).
35. Y. Ohishi, "Novel photonics materials for broadband lightwave processing," in *Photonics West* (SPIE, 2007).